# Estimation of the maximal Lyapunov exponent of nonsmooth systems using chaos synchronization

Michael Baumann[1] and Remco I. Leine[2]

[1]*Institute of Mechanical Systems, ETH Zurich, baumann@imes.mavt.ethz.ch*
[2]*Institute for Nonlinear Mechanics, University of Stuttgart, remco.leine@inm.uni-stuttgart.de*

ABSTRACT — *The maximal Lyapunov exponent of a nonsmooth system is the lower bound for the proportional feedback gain necessary to achieve full state synchronization. In this paper, we prove this statement for the general class of nonsmooth systems in the framework of measure differential inclusions. The results are used to estimate the maximal Lyapunov exponent using chaos synchronization, which is illustrated using a mechanical impact oscillator.*

## 1  Introduction

The spectrum of Lyapunov exponents is an important characteristic of limit sets. It measures the exponential convergence or divergence of nearby trajectories, thereby capturing the sensitivity of solutions with respect to initial conditions [38]. An infinitesimal sphere of perturbed initial conditions will deform into an ellipsoid under the flow of a smooth dynamical system [43]. The Lyapunov exponents capture the average exponential growth or decay rate of the principal axes of the ellipsoid and the maximal Lyapunov exponent captures the long-term behavior of the dominating direction. For example, an attractive limit cycle has only negative Lyapunov exponents (except possibly one at zero corresponding to the freedom of phase [20]). A positive maximal Lyapunov exponent implies instability of the limit set (i.e., equilibrium, limit cycle, periodic or quasi-periodic solution) or it can be an indication for a chaotic attractor [19,21,25].

The existence of the Lyapunov exponents is a subtle question for non-conservative systems [32,40]. The mathematic foundation for the existence is given by the multiplicative ergodic theorem of Oseledec [31] (cf. [37]). It states that, if there exists an invariant measure of the flow, then the Lyapunov exponents exist for almost every point with respect to that measure. For further literature on ergodic theory of differentiable dynamical systems, see [4,12].

Algorithms to find the spectrum of Lyapunov exponents for smooth systems are well established [5, 6, 12]. The spectrum can be computed numerically by linearizing the differential equations along the nominal solution. Time integration of the linearized equations yields the fundamental solution matrix from which the spectrum of Lyapunov exponents can be obtained. Numerical errors during the integration process will always turn any initial error in the maximally expanding direction [21,29] (i.e., the direction corresponding to the maximal Lyapunov exponent), which can be compensated by repeatedly applying a Gram-Schmidt reorthonormalization. The estimation of Lyapunov exponents from experimental time series of systems with unknown dynamics has been presented in [11,17,39,44].

Dynamical systems with a discontinuous right-hand side exhibit discontinuities in the evolution of the fundamental solution matrix. The jumps can be captured using a saltation matrix and the jump conditions for transversal crossings of the discontinuity surfaces are given by the authors of [2] in their study of the stability of periodic motion. The numerical computation of the Lyapunov exponents with jump conditions including the motion on sliding surfaces is shown in [7]. The theory of [2] has been applied to Filippov-type systems in [23] with an emphasis on mechanical systems with Coulomb friction. In [28], a model based algorithm for the calculation of the spectrum of Lyapunov exponents is presented for dynamical systems with discontinuous motion and illustrated using the example of a one-dimensional

mechanical oscillator with Coulomb friction. The method presented in [28] has been applied in [1] to the rocking block example.

Two diffusively coupled identical smooth systems achieve synchronization despite the complicated dynamics of the individual systems if the coupling parameter is large enough [34]. The minimal value of the coupling parameter for which the synchronization set is (attractively) stable is determined by the maximal Lyapunov exponent of the individual systems. This relation arises from the competitive behavior of the separation due to the trajectory instability (dominated by the maximal Lyapunov exponent) and the convergence due to the coupling. Estimating the maximal Lyapunov exponent using the critical coupling necessary for synchronization has been proposed in [15, 45] for continuous nonlinear systems and has been continued in [16, 46], which also includes the study of the behavior after the instability point of synchronized chaos. The relation between the maximal Lyapunov exponent and stable chaos synchronization has been presented in the more recent work [3] in the context of complex networks.

The method of estimating the maximal Lyapunov exponent using chaos synchronization has been considered in [41] for nonsmooth systems and in [42] for discrete maps. In [41, 42], however, the increase of the initial perturbation is assumed to be uniform in time, which is only the case if the Jacobian of the vector field (continuous or discrete) is constant (i.e., for linear time-invariant systems). The application of this method has been presented in [14] for a multi-body system with dry friction.

In this paper, we consider the class of nonsmooth systems with solutions of special locally bounded variation, which can be written in the framework of measure differential inclusions [9, 24, 26, 27]. We prove for this general class of nonsmooth systems that the critical coupling is indeed given by maximal Lyapunov exponent as long as the maximal Lyapunov exponent exists.

The paper is organized as follows. We first restrict ourselves to smooth systems in Section 2 before we state the main result for nonsmooth systems in Section 3. The results are illustrated in Section 4 using a mechanical impact oscillator and conclusions are given in Section 5.

## 2 Smooth systems

The dynamics of a smooth system is given by

$$\frac{\mathrm{d}\boldsymbol{x}}{\mathrm{d}t} = \boldsymbol{f}(\boldsymbol{x}, t), \tag{1}$$

where the vector field $\boldsymbol{f} : \mathbb{R}^n \times \mathbb{R} \to \mathbb{R}^n$ is continuously differentiable in its first argument and continuous in its second argument. We denote the solution of (1) for the initial conditions $\boldsymbol{x}(t_0) = \boldsymbol{x}_0$ as $\boldsymbol{x}(t) = \boldsymbol{\varphi}(t, \boldsymbol{x}_0, t_0)$, where the dependence on initial conditions is written explicitly. We introduce the perturbed solution $(\boldsymbol{x} + \Delta\boldsymbol{x})(t) = \boldsymbol{\varphi}(t, \boldsymbol{x}_0 + \kappa\boldsymbol{e}, t_0)$ obtained using the perturbed initial conditions $\boldsymbol{x}_0 + \kappa\boldsymbol{e}$ with $\|\boldsymbol{e}\| = 1$ and $\kappa > 0$ small. The dynamics of the perturbation $\Delta\boldsymbol{x}(t)$ is obtained as

$$\frac{\mathrm{d}(\Delta\boldsymbol{x})}{\mathrm{d}t} = \boldsymbol{f}(\boldsymbol{x} + \Delta\boldsymbol{x}, t) - \boldsymbol{f}(\boldsymbol{x}, t) = \boldsymbol{A}(t)\Delta\boldsymbol{x} + \boldsymbol{o}\left(\|\Delta\boldsymbol{x}\|\right), \tag{2}$$

where $\boldsymbol{A}(t) := \left.\frac{\partial \boldsymbol{f}(\boldsymbol{x},t)}{\partial \boldsymbol{x}}\right|_{\boldsymbol{\varphi}(t,\boldsymbol{x}_0,t_0)}$ is the linearization of the vector field $\boldsymbol{f}$ along the unperturbed solution and $\boldsymbol{o}$ denotes the (small) Landau-order symbol[1]. The perturbation $\Delta\boldsymbol{x}$ tends to zero for $\kappa \to 0$. Therefore, we introduce the normalized perturbation $\boldsymbol{\xi}(t, \boldsymbol{e}, t_0) := \lim_{\kappa \to 0} \boldsymbol{\xi}_\kappa(t, \boldsymbol{e}, t_0)$, where $\boldsymbol{\xi}_\kappa(t, \boldsymbol{e}, t_0) := \frac{\Delta\boldsymbol{x}}{\|\Delta\boldsymbol{x}_0\|} = \frac{\boldsymbol{\varphi}(t,\boldsymbol{x}_0+\kappa\boldsymbol{e},t_0)-\boldsymbol{\varphi}(t,\boldsymbol{x}_0,t_0)}{\kappa}$. The limit exists because $\boldsymbol{\mathcal{O}}\left(\|\Delta\boldsymbol{x}\|\right) = \boldsymbol{\mathcal{O}}\left(\|\Delta\boldsymbol{x}(t_0)\|\right) = \boldsymbol{\mathcal{O}}\left(\kappa\right)$, where $\boldsymbol{\mathcal{O}}$ denotes

---

[1]The (small) Landau-order symbol $\boldsymbol{o}$ is defined as $\boldsymbol{g}(x) \in \boldsymbol{o}\left(h(x)\right) \Leftrightarrow g_i(x) \in o\left(h(x)\right) \ \forall i \Leftrightarrow \lim_{x \to a} \left|\frac{g_i(x)}{h(x)}\right| = 0 \ \forall i$ with $a \in \overline{\mathbb{R}}$.

the (big) Landau-order symbols[2]. Taking the limit $\kappa \to 0$ of (2), divided by $\kappa$, yields

$$\lim_{\kappa \to 0} \frac{\mathrm{d}\boldsymbol{\xi}_\kappa}{\mathrm{d}t} = \boldsymbol{A}(t)\boldsymbol{\xi}. \tag{3}$$

The vector field $\boldsymbol{f}$ is continuously differentiable in its first argument, which implies local uniform convergence of $\lim_{\kappa \to 0} \frac{\mathrm{d}\boldsymbol{\xi}_\kappa}{\mathrm{d}t}$. Using [36, Theorem 7.17] together with (3) yields

$$\frac{\mathrm{d}\boldsymbol{\xi}}{\mathrm{d}t} = \boldsymbol{A}(t)\boldsymbol{\xi}. \tag{4}$$

Let $\boldsymbol{\Phi}(t, t_0)$ be the fundamental solution matrix, which is the solution to the matrix differential equation $\frac{\mathrm{d}\boldsymbol{\Phi}}{\mathrm{d}t} = \boldsymbol{A}(t)\boldsymbol{\Phi}$ for the initial conditions $\boldsymbol{\Phi}(t_0, t_0) = \boldsymbol{I}$, where $\boldsymbol{I}$ is the identity matrix. Then, the solution of the normalized difference $\boldsymbol{\xi}$ can be written as $\boldsymbol{\xi}(t, \boldsymbol{e}, t_0) = \boldsymbol{\Phi}(t, t_0)\boldsymbol{e}$. Furthermore, let $\sigma_i(\boldsymbol{\Phi}) = \sqrt{\mathrm{eig}_i(\boldsymbol{\Phi}\boldsymbol{\Phi}^\mathsf{T})}$ be the singular values of $\boldsymbol{\Phi}$. The spectrum or Lyapunov exponents is given by $\lambda_i = \lim_{t \to \infty} \frac{1}{t} \ln \sigma_i$, where the maximal Lyapunov exponent is denoted by $\lambda_{\max} = \max_i\{\lambda_i\}$. The largest singular value is the spectral norm, that is, the matrix norm induced by the Euclidean norm. The maximal Lyapunov exponent can therefore be defined by

$$\lambda_{\max} := \max_{\boldsymbol{e}} \lim_{t \to \infty} \frac{1}{t} \ln \|\boldsymbol{\xi}(t, \boldsymbol{e}, t_0)\|. \tag{5}$$

Up to this point, we have discussed the perturbation dynamics of the smooth dynamical system (1) and we have defined the maximal Lyapunov exponent in (5) using the normalized perturbation $\boldsymbol{\xi}$. In the following, we consider the error dynamics of two identical smooth systems with a unidirectional diffuse coupling. For this purpose, system (1) is accompanied by a replica together with a proportional error feedback as

$$\begin{aligned} \frac{\mathrm{d}\boldsymbol{x}}{\mathrm{d}t} &= \boldsymbol{f}(\boldsymbol{x}, t), \\ \frac{\mathrm{d}\boldsymbol{y}}{\mathrm{d}t} &= \boldsymbol{f}(\boldsymbol{y}, t) - k(\boldsymbol{y} - \boldsymbol{x}), \end{aligned} \tag{6}$$

where $k \in \mathbb{R}$ is the coupling gain. The initial conditions are chosen as $\boldsymbol{x}(t_0) = \boldsymbol{x}_0$ and $\boldsymbol{y}(t_0) = \boldsymbol{x}_0 + \kappa\boldsymbol{e}$, which are the same initial conditions as for the perturbation dynamics. Let $\boldsymbol{z} := \boldsymbol{y} - \boldsymbol{x}$ denote the synchronization error of the coupled dynamics (6). Using the linearization $\boldsymbol{A}(t) = \left.\frac{\partial \boldsymbol{f}(\boldsymbol{x}, t)}{\partial \boldsymbol{x}}\right|_{\boldsymbol{\varphi}(t, \boldsymbol{x}_0, t_0)}$, the error dynamics is described by

$$\frac{\mathrm{d}\boldsymbol{z}}{\mathrm{d}t} = \boldsymbol{A}(t)\boldsymbol{z} - k\boldsymbol{z} + \boldsymbol{o}(\|\boldsymbol{z}\|). \tag{7}$$

The error $\boldsymbol{z}$ is of the order of the initial error $\boldsymbol{z}_0$, which itself is proportional to $\kappa$. Analogously to the normalized perturbation $\boldsymbol{\xi}$, we define the normalized synchronization error as $\boldsymbol{\zeta}(t, \boldsymbol{e}, t_0) := \lim_{\kappa \to 0} \frac{\boldsymbol{z}}{\kappa}$. Taking the limit $\kappa \to 0$ of (7), divided by $\kappa$, and using $\boldsymbol{z} \in \mathcal{O}(\kappa)$ yields

$$\frac{\mathrm{d}\boldsymbol{\zeta}}{\mathrm{d}t} = \boldsymbol{A}(t)\boldsymbol{\zeta} - k\boldsymbol{\zeta}. \tag{8}$$

By comparing (4) and (8), we find that

$$\boldsymbol{\zeta} = \boldsymbol{\Phi}(t, t_0)e^{-k(t-t_0)}\boldsymbol{e} = \boldsymbol{\xi}e^{-k(t-t_0)}. \tag{9}$$

---

[2]The (big) Landau-order symbol $\mathcal{O}$ is defined as $\boldsymbol{g}(x) \in \mathcal{O}(h(x)) \Leftrightarrow g_i(x) \in \mathcal{O}(h(x)) \ \forall i \Leftrightarrow \limsup_{x \to a} \left|\frac{g_i(x)}{h(x)}\right| < \infty \ \forall i$ with $a \in \mathbb{R}$.

Local synchronization of the coupled system (6) is achieved if there exists a constant $c > 0$ such that $\lim_{t\to\infty} \|\boldsymbol{z}(t)\| = 0$ $\forall \|\boldsymbol{z}_0\| < c$. Hence, local synchronization is achieved if the limit of the normalized synchronization error $\boldsymbol{\zeta}(t, \boldsymbol{e}, t_0)$ as $t \to \infty$ is zero for all $\boldsymbol{e}$. The 'worst case' of all possible limits can be written using (9) together with (5) as

$$\max_{\boldsymbol{e}} \lim_{t\to\infty} \|\boldsymbol{\zeta}\| = \max_{\boldsymbol{e}} \lim_{t\to\infty} \|\boldsymbol{\xi}\| e^{-k(t-t_0)} = \lim_{t\to\infty} e^{(\lambda_{\max}-k)(t-t_0)},$$

from which follows that local synchronization of the coupled system (6) is achieved if (and only if) the coupling gain $k$ is larger than the maximal Lyapunov exponent $\lambda_{\max}$:

$$\lim_{t\to\infty} \|\boldsymbol{\zeta}(t, \boldsymbol{e}, t_0)\| = 0 \ \forall \boldsymbol{e} \ \text{if and only}^* \text{ if } k > \lambda_{\max}. \tag{10}$$

The star in (10) denotes that $k = \lambda_{\max}$ is excluded in the converse. No statement can be made for the case where $k$ is exactly equal to $\lambda_{\max}$ because, for this case, the stability and attractivity is determined by higher order terms.

**Remark 1.** Every strange attractor has a positive maximal Lyapunov exponent [25, 43] and, thus, a positive critical coupling gain $k_{\text{crit}}$ (i.e., the minimal coupling gain necessary to achieve local synchronization). However, the derived results are also applicable to other limit sets than chaotic attractors. For example, an attractive equilibrium has a negative maximal Lyapunov exponent and thus the critical coupling gain is negative as well.

If the initial conditions are exactly orthogonal to the direction corresponding to the maximal Lyapunov exponent, then the synchronization error can tend to zero for a coupling gain $k$ is smaller than $\lambda_{\max}$. However, any slight error or uncertainty will turn any initial error in the direction of maximal expansion [21, 29], that is,

$$\exists \boldsymbol{e} : \ \lim_{t\to\infty} \|\boldsymbol{\zeta}(t, \boldsymbol{e}, t_0)\| = 0 \quad \Rightarrow \quad \lim_{t\to\infty} \|\boldsymbol{\zeta}(t, \boldsymbol{e}, t_0)\| = 0 \ \text{ for almost all } \boldsymbol{e}.$$

Therefore, in practice, local synchronization is achieved if and only if the coupling gain $k$ is larger than the critical coupling gain $k_{\text{crit}} = \lambda_{\max}$.

## 3 Non-smooth systems

The non-smooth dynamics is written in the form of a measure differential inclusion [9, 24, 26, 27] as

$$\frac{\mathrm{d}\boldsymbol{x}}{\mathrm{d}\mu} \in \boldsymbol{\mathcal{F}}(\boldsymbol{x}, t). \tag{11}$$

The solution for the admissible initial conditions $\boldsymbol{x}^-(t_0) = \boldsymbol{x}_0$ is denoted by $\boldsymbol{x}(t) = \boldsymbol{\varphi}(t, \boldsymbol{x}_0, t_0)$. Solutions are generally discontinuous, but assumed to be of special locally bounded variation. The density $\frac{\mathrm{d}\boldsymbol{x}}{\mathrm{d}\mu}$ in (11) is the density of the measure $\mathrm{d}\boldsymbol{x}$ with respect to a positive Radon measure $\mathrm{d}\mu$ and, according to [8, Theorem 5.8.8][3], can be defined as

$$\frac{\mathrm{d}\boldsymbol{x}}{\mathrm{d}\mu}(t) := \lim_{\varepsilon\to 0} \frac{\mathrm{d}\boldsymbol{x}(I_\varepsilon)}{\mathrm{d}\mu(I_\varepsilon)}, \tag{12}$$

where $I_\varepsilon(t) := (t-\varepsilon, t+\varepsilon)$ with $\varepsilon > 0$ is the open time interval centered at $t$. The solutions are absolutely continuous almost everywhere (a.e.) (i.e., for almost all $t \in \mathbb{R}$ with respect to the Lebesgue measure)

---

[3]Theorem 5.8.8 in [8] considers closed intervals (closed balls), but the interval $I_\varepsilon$ are open. The theorem is nevertheless applicable since every Radon measure is regular on a $\sigma$-compact Hausdorff space (here, $\mathbb{R}$ equipped with the standard topology) according to [13, Chapter 8, Corollary 1.13].

and have at most countably many discontinuities, at which the solutions are undefined. However, the one-sided limits $\boldsymbol{x}^-(t) = \lim_{\tau \to 0, \tau < 0} \boldsymbol{x}(t + \tau)$ and $\boldsymbol{x}^+(t) = \lim_{\tau \to 0, \tau > 0} \boldsymbol{x}(t + \tau)$ are well defined on the entire time axis.

As for the smooth case in Section 2, we consider a reference solution $\boldsymbol{x}(t) = \boldsymbol{\varphi}(t, \boldsymbol{x}_0, t_0)$ and a perturbed solution $(\boldsymbol{x} + \Delta \boldsymbol{x})(t) = \boldsymbol{\varphi}(t, \boldsymbol{x}_0 + \kappa \boldsymbol{e}, t_0)$ for system (11), where the initial conditions $\boldsymbol{x}_0 + \kappa \boldsymbol{e}$ with $\|\boldsymbol{e}\| = 1$ an $\kappa > 0$ are assumed to be admissible for all $\kappa \geq 0$. Furthermore, we define the normalized perturbation as $\boldsymbol{\xi}(t, \boldsymbol{e}, t_0) := \lim_{\kappa \to 0, \kappa \notin E_\kappa^\xi(t)} \boldsymbol{\xi}_\kappa(t, \boldsymbol{e}, t_0)$, where $\boldsymbol{\xi}_\kappa(t, \boldsymbol{e}, t_0) := \frac{\Delta \boldsymbol{x}}{\kappa}$ and $E_\kappa^\xi(t) := \{\kappa \in \mathbb{R}_0^+ \,|\, \boldsymbol{\xi}_\kappa^-(t, \boldsymbol{e}, t_0) \neq \boldsymbol{\xi}_\kappa^+(t, \boldsymbol{e}, t_0)\}$. To ensure that the normalized perturbation exists a.e., we will make the following assumption.

**Assumption 1.** The difference between two solutions of system (11) is almost everywhere of the order of the initial difference, that is, $\boldsymbol{\varphi}(t, \boldsymbol{x}_0 + \kappa \boldsymbol{e}, t_0) - \boldsymbol{\varphi}(t, \boldsymbol{x}_0, t_0) \in \mathcal{O}(\kappa)$ a.e.

Assumption 1 together with $\mathcal{O}(\kappa) \subset \boldsymbol{o}(1)$ implies continuous dependence on initial conditions, which can be written as $\lim_{\kappa \to 0} \boldsymbol{\varphi}(t, \boldsymbol{x}_0 + \kappa \boldsymbol{e}, t_0) - \boldsymbol{\varphi}(t, \boldsymbol{x}_0, t_0) = \boldsymbol{0} \; \forall \boldsymbol{e}$. Furthermore, continuous dependence on initial conditions implies uniqueness of solutions in forward time.

**Remark 2.** Assumption 1 is generally restrictive for non-smooth systems. For example, mechanical systems subjected to frictionless unilateral constraints do generally not have continuity on initial conditions [33]. Furthermore, the stated assumption does omit grazing trajectories (i.e., 'collisions' with zero relative velocity) because the Poincaré map at a grazing trajectory has an infinite slope (due to a square-root term in the Poincaré map [10, 30]). Assumption 1 does, however, allow for accumulation points, which is a phenomenon describing (countably) infinitely many impact events in a finite time interval.

If Assumption 1 is not met, then the normalized difference $\boldsymbol{\xi}(t, \boldsymbol{e}, t_0)$ tends (or jumps) to infinity in finite time. In this case, the maximal Lyapunov exponent does not exist and, considering two identical, coupled systems, no local synchronization can be achieved with a finite coupling gain $k$.

If the unperturbed solution has a discontinuity at time $t$, then the one-sided limits of $\boldsymbol{\varphi}(t, \boldsymbol{x}_0 + \kappa \boldsymbol{e}, t_0) - \boldsymbol{\varphi}(t, \boldsymbol{x}_0, t_0)$ are not necessarily of order $\mathcal{O}(\kappa)$, because the discontinuities of $\boldsymbol{\varphi}(t, \boldsymbol{x}_0 + \kappa \boldsymbol{e}, t_0)$ and $\boldsymbol{\varphi}(t, \boldsymbol{x}_0, t_0)$ do generally not occur at the same points in time for $\kappa > 0$. However, Assumption 1 implies that the discontinuity points of $\boldsymbol{\varphi}(t, \boldsymbol{x}_0 + \kappa \boldsymbol{e}, t_0)$ tend to the ones of $\boldsymbol{\varphi}(t, \boldsymbol{x}_0, t_0)$ such that $\boldsymbol{\xi}$ exist for almost all $t \in \mathbb{R}$, which is illustrated in Figure 1. It shows an unperturbed solution $\boldsymbol{\varphi}(t, \boldsymbol{x}_0, t_0)$ with a discontinuity at $t = 1$ and a kink at $t = 5$. The perturbed solutions $\boldsymbol{\varphi}(t, \boldsymbol{x}_0 + \kappa \boldsymbol{e}, t_0)$ tend almost everywhere to the unperturbed solutions for $\kappa \to 0$, that is, $\lim_{\kappa \to 0} \Delta \boldsymbol{x} = \boldsymbol{0}$ a.e. The jump in $\boldsymbol{\varphi}$ yields a peak in the normalized perturbation $\boldsymbol{\xi}$ (i.e., $\boldsymbol{\xi}$ is undefined at this point) and the kink in $\boldsymbol{\varphi}$ yields a jump in $\boldsymbol{\xi}$. Therefore, due to Assumption 1, the normalized perturbation $\boldsymbol{\xi}(t, \boldsymbol{e}, t_0)$ exists for almost all $t$.

Since (11) has a unique solution in forward time by Assumption 1, the density $\frac{\mathrm{d}\boldsymbol{x}}{\mathrm{d}\mu}$ is unique as well and the dynamics can be written as a measure differential equation

$$\frac{\mathrm{d}\boldsymbol{x}}{\mathrm{d}\mu} = \boldsymbol{f}(\boldsymbol{x}^-, t), \tag{13}$$

where $\boldsymbol{f}(\boldsymbol{x}^-, t) \in \mathcal{F}(\boldsymbol{x}, t)$.

The dynamics of the perturbation $\Delta \boldsymbol{x}$ is governed by $\frac{\mathrm{d}\Delta \boldsymbol{x}}{\mathrm{d}\mu} = \boldsymbol{f}(\boldsymbol{x}^- + \Delta \boldsymbol{x}^-, t) - \boldsymbol{f}(\boldsymbol{x}^-, t)$. Dividing by $\kappa$ and substituting the definition of $\boldsymbol{\xi}_\kappa$ yields

$$\frac{\mathrm{d}\boldsymbol{\xi}_\kappa}{\mathrm{d}\mu} = \frac{\boldsymbol{f}(\boldsymbol{x}^- + \kappa \boldsymbol{\xi}_\kappa^-, t) - \boldsymbol{f}(\boldsymbol{x}^-, t)}{\kappa}. \tag{14}$$

The density $\frac{\mathrm{d}\boldsymbol{\xi}_\kappa}{\mathrm{d}\mu}$ does not uniformly converge to $\frac{\mathrm{d}\boldsymbol{\xi}}{\mathrm{d}\mu}$ for $\kappa \to 0$ at the discontinuity points. This is the case because the discontinuities of $\boldsymbol{\varphi}(t, \boldsymbol{x}_0 + \kappa \boldsymbol{e}, t_0)$ and $\boldsymbol{\varphi}(t, \boldsymbol{x}_0, t_0)$ do generally not coincide (see illustrative example depicted in Figure 1 at $t = 1$). Therefore, we cannot simply take the limit of (14) as $\kappa \to 0$. In
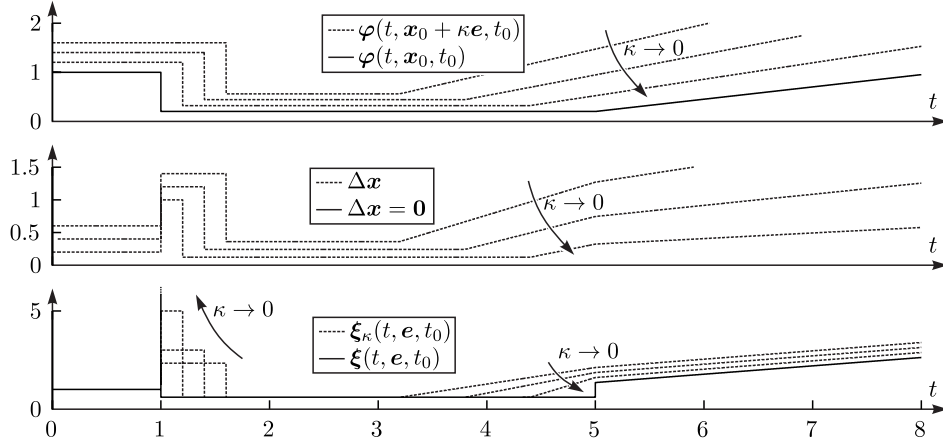
Fig. 1: Assumption 1 implies that the normalized perturbation $\boldsymbol{\xi}(t, \boldsymbol{e}, t_0)$ exists for almost all $t$.

order to deal with this problem, we do not consider the density $\frac{\mathrm{d}\boldsymbol{\xi}_\kappa}{\mathrm{d}\mu}$ for a singleton $\{t\}$, but rather on an open time interval $I_\varepsilon(t) = (t - \varepsilon, \, t + \varepsilon)$ with $\varepsilon > 0$. Using the notation $(\boldsymbol{f} \odot \mathrm{d}\mu)(I_\varepsilon) = \int_{I_\varepsilon} \boldsymbol{f}\mathrm{d}\mu$ [13], the 'widened' density $\frac{\mathrm{d}\boldsymbol{\xi}_\kappa}{\mathrm{d}\mu}$ for the interval $I_\varepsilon$ is obtained as

$$\frac{\mathrm{d}\boldsymbol{\xi}_\kappa(I_\varepsilon)}{\mathrm{d}\mu(I_\varepsilon)} = \frac{(\boldsymbol{f}(\boldsymbol{x}^- + \kappa\boldsymbol{\xi}_\kappa^-, t) \odot \mathrm{d}\mu)(I_\varepsilon) - (\boldsymbol{f}(\boldsymbol{x}^-, t) \odot \mathrm{d}\mu)(I_\varepsilon)}{\kappa\,\mathrm{d}\mu(I_\varepsilon)}. \tag{15}$$

The right-hand side of (15) can be considered as the time average over the interval $I_\varepsilon$ of the one-sided directional derivative of $\boldsymbol{f}$ in the direction of $\boldsymbol{\xi}_\kappa^-$. The vector field $\boldsymbol{f}$ is non-differentiable and not even semidifferentiable [35]. In the following, we show that the one-sided directional derivative is nevertheless well-defined if the solution and its perturbation is not discontinuous on the boundary of the open time interval $I_\varepsilon$. Therefore, we rewrite (15) as

$$\frac{\mathrm{d}\boldsymbol{\xi}_\kappa(I_\varepsilon)}{\mathrm{d}\mu(I_\varepsilon)} = \frac{(\boldsymbol{f}(\boldsymbol{x}^- + \kappa\boldsymbol{\xi}_\kappa^-, t) \odot \mathrm{d}\mu)([t_0, \, t + \varepsilon) \setminus [t_0, \, t - \varepsilon]) - (\boldsymbol{f}(\boldsymbol{x}^-, t) \odot \mathrm{d}\mu)([t_0, \, t + \varepsilon) \setminus [t_0, \, t - \varepsilon])}{\kappa\,\mathrm{d}\mu(I_\varepsilon)}$$

$$= \frac{(\boldsymbol{\varphi}^-(t + \varepsilon, \boldsymbol{x}_0 + \kappa\boldsymbol{e}, t_0) - \boldsymbol{\varphi}^+(t - \varepsilon, \boldsymbol{x}_0 + \kappa\boldsymbol{e}, t_0)) - (\boldsymbol{\varphi}^-(t + \varepsilon, \boldsymbol{x}_0, t_0) - \boldsymbol{\varphi}^+(t - \varepsilon, \boldsymbol{x}_0, t_0))}{\kappa\,\mathrm{d}\mu(I_\varepsilon)}$$

$$= \frac{1}{\mathrm{d}\mu(I_\varepsilon)} \frac{\boldsymbol{\varphi}^-(t + \varepsilon, \boldsymbol{x}_0 + \kappa\boldsymbol{e}, t_0) - \boldsymbol{\varphi}^-(t + \varepsilon, \boldsymbol{x}_0, t_0)}{\kappa}$$

$$- \frac{1}{\mathrm{d}\mu(I_\varepsilon)} \frac{\boldsymbol{\varphi}^+(t - \varepsilon, \boldsymbol{x}_0 + \kappa\boldsymbol{e}, t_0) - \boldsymbol{\varphi}^+(t - \varepsilon, \boldsymbol{x}_0, t_0)}{\kappa}.$$

The limits $\lim_{\kappa \to 0, \kappa \notin E_\kappa^\xi(t+\varepsilon)} \frac{\boldsymbol{\varphi}^-(t+\varepsilon, \boldsymbol{x}_0+\kappa\boldsymbol{e}, t_0) - \boldsymbol{\varphi}^-(t+\varepsilon, \boldsymbol{x}_0, t_0)}{\kappa}$ and $\lim_{\kappa \to 0, \kappa \notin E_\kappa^\xi(t-\varepsilon)} \frac{\boldsymbol{\varphi}^+(t-\varepsilon, \boldsymbol{x}_0+\kappa\boldsymbol{e}, t_0) - \boldsymbol{\varphi}^+(t-\varepsilon, \boldsymbol{x}_0, t_0)}{\kappa}$ exist according to Assumption 1 as long as the solution $\boldsymbol{\varphi}$ is not discontinuous on the boundary of $I_\varepsilon$. Considering only values of $\varepsilon \notin E_\varepsilon^\varphi := \{\varepsilon \in \mathbb{R}^+ \,|\, \boldsymbol{\varphi}^-(t - \varepsilon, \boldsymbol{x}_0, t_0) \neq \boldsymbol{\varphi}^+(t - \varepsilon, \boldsymbol{x}_0, t_0) \vee \boldsymbol{\varphi}^-(t + \varepsilon, \boldsymbol{x}_0, t_0) \neq \boldsymbol{\varphi}^+(t + \varepsilon, \boldsymbol{x}_0, t_0)\}$, we obtain $\lim_{\kappa \to 0, \kappa \notin E_\kappa^\xi(t\pm\varepsilon)} \frac{\mathrm{d}\boldsymbol{\xi}_\kappa(I_\varepsilon)}{\mathrm{d}\mu(I_\varepsilon)} = \frac{\mathrm{d}\boldsymbol{\xi}(I_\varepsilon)}{\mathrm{d}\mu(I_\varepsilon)}$, where $E_\kappa^\xi(t \pm \varepsilon) = E_\kappa^\xi(t - \varepsilon) \cup E_\kappa^\xi(t + \varepsilon)$.

In the following step, we let $\varepsilon$ tend to zero while omitting the values $\varepsilon \in E_\varepsilon^\varphi$ and use $\lim_{\varepsilon \to 0} I_\varepsilon = \{t\}$ and (12) to obtain $\lim_{\varepsilon \to 0, \varepsilon \notin E_\varepsilon^\varphi} \frac{\mathrm{d}\boldsymbol{\xi}(I_\varepsilon)}{\mathrm{d}\mu(I_\varepsilon)} = \frac{\mathrm{d}\boldsymbol{\xi}}{\mathrm{d}\mu}$. Together with (15), the density $\frac{\mathrm{d}\boldsymbol{\xi}}{\mathrm{d}\mu}$ is obtained as

$$\frac{\mathrm{d}\boldsymbol{\xi}}{\mathrm{d}\mu} = \lim_{\varepsilon \to 0, \varepsilon \notin E_\varepsilon^\varphi} \lim_{\kappa \to 0, \kappa \notin E_\kappa^\xi(t\pm\varepsilon)} \frac{(\boldsymbol{f}(\boldsymbol{x}^- + \kappa\boldsymbol{\xi}^-, t) \odot \mathrm{d}\mu)(I_\varepsilon) - (\boldsymbol{f}(\boldsymbol{x}^-, t) \odot \mathrm{d}\mu)(I_\varepsilon)}{\kappa\,\mathrm{d}\mu(I_\varepsilon)}. \tag{16}$$

**Remark 3.** The solution to (16) generally cannot be written using a fundamental solution matrix $\boldsymbol{\Phi}(t, t_0)$ in the form $\boldsymbol{\xi}(t, \boldsymbol{e}, t_0) = \boldsymbol{\Phi}(t, t_0)\boldsymbol{e}$. The reason is not the discontinuous behavior of $\boldsymbol{\xi}$ as this can be

6

captured using a discontinuous fundamental solution matrix as $\boldsymbol{\xi}^+(t, \boldsymbol{e}, t_0) - \boldsymbol{\xi}^-(t, \boldsymbol{e}, t_0) = \boldsymbol{S}(t, t_0)\boldsymbol{e}$, where $\boldsymbol{S}(t, t_0) := \boldsymbol{\Phi}^+(t, t_0) - \boldsymbol{\Phi}^-(t, t_0)$ is referred to as *saltation matrix*. The use of a fundamental solution matrix implies $\boldsymbol{\xi}(t, -\boldsymbol{e}, t_0) = -\boldsymbol{\xi}(t, \boldsymbol{e}, t_0)$, which does generally not hold for non-smooth systems.

Similarly to (5) in the smooth case, we use the normalized perturbation $\boldsymbol{\xi}$ to define the maximal Lyapunov exponent for a non-smooth system as

$$\lambda_{\max} := \max_{\boldsymbol{e}} \limsup_{t \to \infty, t \notin E_t^{\xi}} \frac{1}{t} \ln \|\boldsymbol{\xi}(t, \boldsymbol{e}, t_0)\|, \tag{17}$$

where $E_t^{\xi}$ is the discontinuity set of $\boldsymbol{\xi}$.

In the following, we consider the synchronization problem in order to compare the maximal Lyapunov exponent to the critical coupling gain. The coupled dynamics consists of the non-smooth system (13) and a replica with an error feedback of the form

$$\begin{aligned}
\frac{\mathrm{d}\boldsymbol{x}}{\mathrm{d}\mu} &= \boldsymbol{f}(\boldsymbol{x}^-, t), \\
\frac{\mathrm{d}\boldsymbol{y}}{\mathrm{d}\mu} &= \boldsymbol{f}(\boldsymbol{y}^-, t) - k(\boldsymbol{y} - \boldsymbol{x})\frac{\mathrm{d}t}{\mathrm{d}\mu}.
\end{aligned} \tag{18}$$

The error feedback with the coupling gain $k \in \mathbb{R}$ has only a density with respect to the Lebesgue measure $\mathrm{d}t$ because we do not consider any impulsive feedback.

**Remark 4.** The coupled dynamics (18) does not generally arise from (11) accompanied with $\frac{\mathrm{d}\boldsymbol{y}}{\mathrm{d}\mu} \in \mathcal{F}(\boldsymbol{y}, t) - k(\boldsymbol{y} - \boldsymbol{x})\frac{\mathrm{d}t}{\mathrm{d}\mu}$, because the (unique) selection $\boldsymbol{f}(\boldsymbol{y}^-, t) \in \mathcal{F}(\boldsymbol{y}, t)$ is generally influenced by the coupling term.

The same initial conditions as for the perturbation $\Delta\boldsymbol{x}$ are chosen, that is, $\boldsymbol{x}^-(t_0) = \boldsymbol{x}_0$ and $\boldsymbol{y}^-(t_0) = \boldsymbol{x}_0 + \kappa\boldsymbol{e}$. The dynamics of the synchronization error $\boldsymbol{z} = \boldsymbol{y} - \boldsymbol{x}$ is obtained as

$$\frac{\mathrm{d}\boldsymbol{z}}{\mathrm{d}\mu} = \boldsymbol{f}(\boldsymbol{x}^- + \boldsymbol{z}^-, t) - \boldsymbol{f}(\boldsymbol{x}^-, t) - k\boldsymbol{z}\frac{\mathrm{d}t}{\mathrm{d}\mu}. \tag{19}$$

Analogously to the smooth case, let the normalized synchronization error be defined as $\boldsymbol{\zeta}(t, \boldsymbol{e}, t_0) := \lim_{\kappa \to 0, \kappa \notin E_\kappa^\zeta(t)} \boldsymbol{\zeta}_\kappa(t, \boldsymbol{e}, t_0)$, where $\boldsymbol{\zeta}_\kappa(t, \boldsymbol{e}, t_0) := \frac{\boldsymbol{z}}{\kappa}$ and $E_\kappa^\zeta(t) := \{\kappa \in \mathbb{R}_0^+ \,|\, \boldsymbol{\zeta}_\kappa^-(t, \boldsymbol{e}, t_0) \neq \boldsymbol{\zeta}_\kappa^+(t, \boldsymbol{e}, t_0)\}$. The limit $\boldsymbol{\zeta}$ exists a.e. according to Assumption 1. It will prove advantageous to introduce $\hat{\boldsymbol{\zeta}}_\kappa := \boldsymbol{\zeta}_\kappa e^{k(t-t_0)}$ together with its limit $\hat{\boldsymbol{\zeta}} = \lim_{\kappa \to 0, \kappa \notin E_\kappa^{\hat\zeta}(t)} \hat{\boldsymbol{\zeta}}_\kappa = \boldsymbol{\zeta} e^{k(t-t_0)}$. The density of $\hat{\boldsymbol{\zeta}}_\kappa$ w.r.t. $\mathrm{d}\mu$ is obtained from (19) as

$$\frac{\mathrm{d}\hat{\boldsymbol{\zeta}}_\kappa}{\mathrm{d}\mu} = \frac{\boldsymbol{f}(\boldsymbol{x}^- + \kappa\, e^{-k(t-t_0)}\hat{\boldsymbol{\zeta}}_\kappa^-, t) - \boldsymbol{f}(\boldsymbol{x}^-, t)}{\kappa\, e^{-k(t-t_0)}}, \tag{20}$$

where $\frac{\mathrm{d}(\hat{\boldsymbol{\zeta}}_\kappa e^{-k(t-t_0)})}{\mathrm{d}\mu} = \frac{\mathrm{d}(\hat{\boldsymbol{\zeta}}_\kappa)}{\mathrm{d}\mu} e^{-k(t-t_0)} - k\hat{\boldsymbol{\zeta}}_\kappa e^{-k(t-t_0)}\frac{\mathrm{d}t}{\mathrm{d}\mu}$ has been used. As for the normalized perturbation, we cannot directly take the limit of (20) for $\kappa \to 0$. Therefore, the same steps as performed between (14) and (16) are applied to (20) in order to obtain the density $\frac{\mathrm{d}\hat{\boldsymbol{\zeta}}}{\mathrm{d}\mu}$ as

$$\frac{\mathrm{d}\hat{\boldsymbol{\zeta}}}{\mathrm{d}\mu} = \lim_{\varepsilon \to 0, \varepsilon \notin E_\varepsilon^\varphi} \lim_{\kappa \to 0, \kappa \notin E_\kappa^{\hat\zeta}(t\pm\varepsilon)} \frac{\left(\boldsymbol{f}(\boldsymbol{x}^- + \kappa\, e^{-k(t-t_0)}\hat{\boldsymbol{\zeta}}^-, t) \odot \mathrm{d}\mu\right)(I_\varepsilon) - \left(\boldsymbol{f}(\boldsymbol{x}^-, t) \odot \mathrm{d}\mu\right)(I_\varepsilon)}{\kappa\, e^{-k(t-t_0)}\, \mathrm{d}\mu(I_\varepsilon)}. \tag{21}$$

Due to $e^{-k(t-t_0)} > 0 \ \forall t \in \mathbb{R}$, we can replace $\kappa$ in (21) by $\hat{\kappa} = \kappa\, e^{-k(t-t_0)} > 0$ and obtain

$$\frac{\mathrm{d}\hat{\boldsymbol{\zeta}}}{\mathrm{d}\mu} = \lim_{\varepsilon \to 0, \varepsilon \notin E_\varepsilon^\varphi} \lim_{\hat\kappa \to 0, \hat\kappa \notin E_{\hat\kappa}^{\hat\zeta}(t\pm\varepsilon)} \frac{\left(\boldsymbol{f}(\boldsymbol{x}^- + \hat{\kappa}\hat{\boldsymbol{\zeta}}^-, t) \odot \mathrm{d}\mu\right)(I_\varepsilon) - \left(\boldsymbol{f}(\boldsymbol{x}^-, t) \odot \mathrm{d}\mu\right)(I_\varepsilon)}{\hat{\kappa}\, \mathrm{d}\mu(I_\varepsilon)}. \tag{22}$$

7

The initial perturbation $\Delta \boldsymbol{x}^-(t_0) = \kappa \boldsymbol{e}$ and the initial synchronization error $\boldsymbol{z}^-(t_0) = \kappa \boldsymbol{e}$ are identical and, thus, the initial normalized perturbation $\boldsymbol{\xi}^-(t_0, \boldsymbol{e}, t_0) = \boldsymbol{e}$ and the initial normalized synchronization error $\boldsymbol{\zeta}^-(t_0, \boldsymbol{e}, t_0) = \boldsymbol{e}$ are identical as well. Together with $\hat{\boldsymbol{\zeta}}^-(t_0, \boldsymbol{e}, t_0) = \boldsymbol{\zeta}^-(t_0, \boldsymbol{e}, t_0)e^{k(t_0-t_0)} = \boldsymbol{e}$ we obtain that the initial conditions of $\boldsymbol{\xi}$ and $\hat{\boldsymbol{\zeta}}$ are identical. Furthermore, the dynamics of $\boldsymbol{\xi}$, given by (16), and the dynamics of $\hat{\boldsymbol{\zeta}}$, given by (22), are identical as well, which yields $\boldsymbol{\xi}(t, \boldsymbol{e}, t_0) = \hat{\boldsymbol{\zeta}}(t, \boldsymbol{e}, t_0)$ a.e. Therefore, using $\boldsymbol{\zeta}(t, \boldsymbol{e}, t_0) = \hat{\boldsymbol{\zeta}}(t, \boldsymbol{e}, t_0)e^{-k(t-t_0)}$, the relation between the normalized disturbance $\boldsymbol{\xi}$ and the normalized synchronization error $\boldsymbol{\zeta}$ is obtained as

$$\boldsymbol{\zeta} = \boldsymbol{\xi} e^{-k(t-t_0)} \quad \text{a.e.} \tag{23}$$

Furthermore, the set of discontinuities $E_t^{\xi}$ of $\boldsymbol{\xi}$ and $E_t^{\zeta}$ of $\boldsymbol{\zeta}$ coincide. The only difference between the non-smooth result (23) and the smooth result (9) is that $\boldsymbol{\zeta}$ and $\boldsymbol{\xi}$ are discontinuous in the non-smooth case and, thus, not defined on the entire time axis.

From (23) together with the definition of the maximal Lyapunov exponent in (17) we obtain the maximal increase of an infinitesimal disturbance along solutions as

$$\max_{\boldsymbol{e}} \lim_{t\to\infty, t\notin E_t^{\zeta}} \|\boldsymbol{\zeta}\| = \max_{\boldsymbol{e}} \lim_{t\to\infty, t\notin E_t^{\xi}} \|\boldsymbol{\xi}\| e^{-k(t-t_0)} = \lim_{t\to\infty} e^{(\lambda_{\max}-k)(t-t_0)}.$$

Local synchronization of the coupled systems (18) is therefore achieved if (and only if) the coupling gain $k$ is larger than the maximal Lyapunov exponent $\lambda_{\max}$, that is,

$$\lim_{t\to\infty, t\notin E_t^{\zeta}} \|\boldsymbol{\zeta}(t, \boldsymbol{e}, t_0)\| = 0 \ \forall \boldsymbol{e} \text{ if and only}^* \text{ if } k > \lambda_{\max}. \tag{24}$$

The star in (24) denotes that $k = \lambda_{\max}$ is excluded in the converse, because, as in the smooth case, no statement can be made for the case where $k$ is exactly equal to $\lambda_{\max}$.

**Remark 5.** In the case of finite time convergence or superstable limit sets [43] (e.g., an accumulation point for a one-dimensional mechanical system) the decay of any initial perturbation is faster than exponential. The maximal Lyapunov exponent for these limit sets is equal to $-\infty$. Therefore, the synchronization gain $k$ can be chosen negative and arbitrarily large and still achieve local synchronization. However, the result (24) is only applicable as long as the synchronization error is small.

As for the smooth case, any slight error or uncertainty will eventually turn any initial error in the direction of maximal expansion, which yields

$$\exists \boldsymbol{e}: \lim_{t\to\infty, t\notin E_t^{\zeta}} \|\boldsymbol{\zeta}(t, \boldsymbol{e}, t_0)\| = 0 \quad \Rightarrow \quad \lim_{t\to\infty, t\notin E_t^{\zeta}} \|\boldsymbol{\zeta}(t, \boldsymbol{e}, t_0)\| = 0 \text{ for almost all } \boldsymbol{e}.$$

Therefore, the maximal Lyapunov exponent can be estimated using the minimal proportional feedback gain for which synchronization is achieved, that is, $k_{\text{crit}} = \lambda_{\max}$.

# 4 Numerical example

We apply the method of estimating the maximal Lyapunov exponent using chaos synchronization to the example of a mechanical Duffing-oscillator with two geometric unilateral constraints as depicted in Figure 2. The state vector $\boldsymbol{x} = \begin{pmatrix} q, & u \end{pmatrix}^{\mathsf{T}}$ consists of the coordinate $q$ and velocity $u$. The impact oscillator is excited by an external, harmonic forcing $f_0 \cos(\omega t)$. The further system parameters are the mass $m$, the nonlinear stiffness coefficient $k(q) = \bar{k}(q^2 - 1)$ and the viscous damping coefficient $d$.

The opposing unilateral constraints located at $q = \pm q_c$ can be written as $\boldsymbol{g} = \begin{pmatrix} q + q_c, & -q + q_c \end{pmatrix}^{\mathsf{T}} \geq \boldsymbol{0}$, which yields $\mathcal{C} = [-q_c, q_c]$ as the admissible set for $q$. The force directions the corresponding constraint forces $\boldsymbol{\lambda}$ and constraint impulses $\boldsymbol{\Lambda}$ are given by $\boldsymbol{W} = \frac{\mathrm{d}\boldsymbol{g}}{\mathrm{d}q}^{\mathsf{T}}$. The force law is given by Signorini's condition
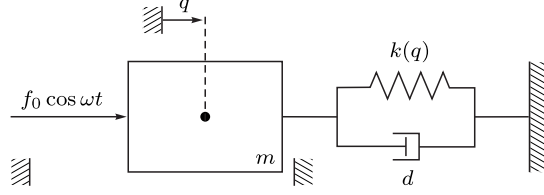
Fig. 2: Duffing oscillator with two opposing geometric unilateral constraints.

and the generalized Newton's impact law with a restitution coefficient $e$ is chosen to describe the impact process [18].

The Radon measure $\mathrm{d}\mu$ is decomposed in a Lebesgue measure $\mathrm{d}t$ and an atomic measure $\mathrm{d}\eta = \sum_i \mathrm{d}\delta_{t_i}$, which is the sum of Dirac point measures $\mathrm{d}\delta_{t_i}$ at the discontinuity points $t_i$ [18]. The dynamics can be written in the form of a measure differential inclusion (11) as

$$\frac{\mathrm{d}\boldsymbol{x}}{\mathrm{d}\mu} = \begin{pmatrix} u\frac{\mathrm{d}t}{\mathrm{d}\mu} \\ \frac{1}{m}\left(-d\,u - \bar{k}\left(q^2 - 1\right)q + f_0 \cos\left(\omega t\right)\right)\frac{\mathrm{d}t}{\mathrm{d}\mu} + \frac{1}{m}\boldsymbol{W}\boldsymbol{P} \end{pmatrix}, \tag{25}$$

where $\boldsymbol{P} = \left\{\boldsymbol{\lambda}\frac{\mathrm{d}t}{\mathrm{d}\mu} + \boldsymbol{\Lambda}\frac{\mathrm{d}\eta}{\mathrm{d}\mu} \mid -\boldsymbol{\lambda} \in \mathcal{N}_{\mathbb{R}_0^+}(\boldsymbol{g}),\ -\boldsymbol{\Lambda} \in \mathcal{H}_q\left(\frac{1}{2}\left(\dot{\boldsymbol{g}}^+ + \dot{\boldsymbol{g}}^-\right)\right)\right\}$. The sets $\mathcal{N}_{\mathbb{R}_0^+}$ and $\mathcal{H}_q$ are used to describe the force and impact laws and are further discussed in [22]. The dynamics described by the measure differential inclusion (25) can be written in the explicit form (13) as

$$\frac{\mathrm{d}\boldsymbol{x}}{\mathrm{d}\mu} = \begin{pmatrix} u\frac{\mathrm{d}t}{\mathrm{d}\mu} \\ \frac{1}{m}\operatorname{prox}_{\mathcal{T}_\mathcal{C}(q)}\left(-d\,u - \bar{k}\left(q^2 - 1\right)q + f_0 \cos\left(\omega t\right)\right)\frac{\mathrm{d}t}{\mathrm{d}\mu} + (1+e)\left(\operatorname{prox}_{\mathcal{T}_\mathcal{C}(q)}\left(u^-\right) - u^-\right)\frac{\mathrm{d}\eta}{\mathrm{d}\mu} \end{pmatrix},$$

where $\operatorname{prox}_{\mathcal{T}_\mathcal{C}(q)}$ is the proximal point function to the tangent cone

$$\mathcal{T}_\mathcal{C}(q) = \begin{cases} \mathbb{R}_0^+ & \text{for } -q_c = q, \\ \mathbb{R} & \text{for } -q_c < q < q_c, \\ \mathbb{R}_0^- & \text{for } \qquad q = q_c. \end{cases}$$

The viscous damping coefficient $d$ is chosen as bifurcation parameter. A brute force diagram is generated for the system parameters $m = \bar{k} = f_0 = \omega = 1, q_c = 0.5, e = 0.65$ for the range $d \in [0, 2.3]$ and is depicted in Figure 3 (top). It is generated using a sweep down of the bifurcation parameter and shows the position $q_P^k$ at the Poincaré sections (here, stroboscopic map with period time $T = \frac{2\pi}{\omega}$). The critical coupling is determined numerically for the solutions depicted in the bifurcation diagram. The critical coupling is used as estimate of the maximal Lyapunov exponent of the corresponding solution and is depicted in Figure 3 (bottom). The estimated maximal Lyapunov exponent is positive for the chaotic attractors and negative ($\lambda_{\max}$ at zero is not considered) during the periodic windows. The coupled system is considered to be synchronized if the synchronization error becomes smaller than a certain threshold and a finite time horizon is chosen in order that the algorithm terminates. Therefore, the maximal Lyapunov exponent is generally overestimated, especially for small values of the damping coefficient $d$.

## 5   Conclusions

The critical coupling gain for local synchronization of two identical nonsmooth systems with unidirectional diffuse coupling is given by the maximal Lyapunov exponent. This statement holds for the general class of nonsmooth systems with solutions of special locally bounded variation under the assumption that the maximal Lyapunov exponent exists.
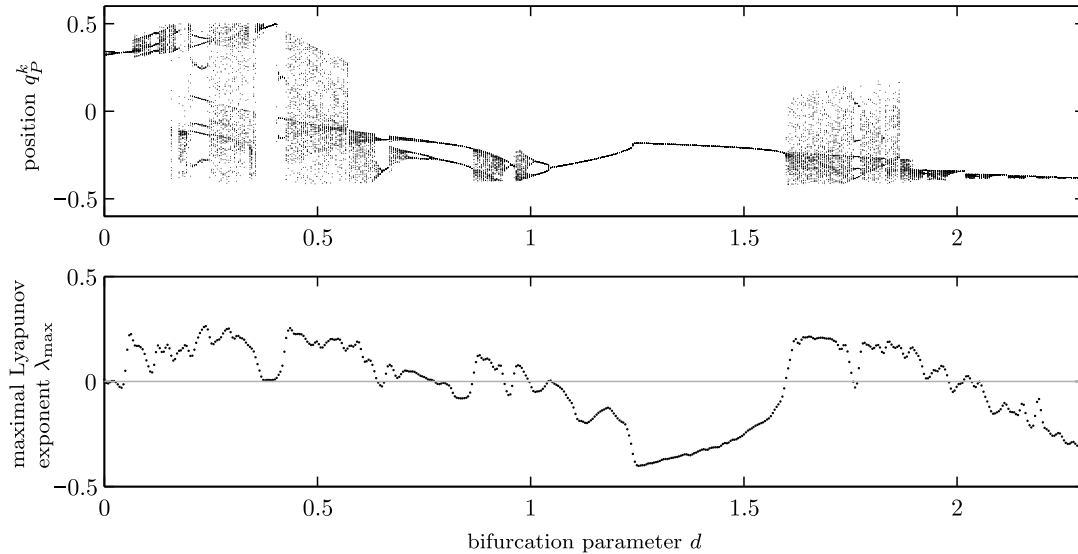
Fig. 3: Brute force diagram (top) and estimation of the maximal Lyapunov exponent $\lambda_{\max}$ (bottom) with the viscous damping coefficient $d$ as bifurcation parameter. The chaotic solutions correspond to $\lambda_{\max} > 0$, while the periodic windows correspond to $\lambda_{\max} < 0$.

The maximal Lyapunov exponent can directly be estimated using chaos synchronization in computer simulations. Using this method in an experimental setup would require a mutual coupling for which the critical coupling gain is half the critical coupling gain compared to unidirectional coupling. However, an experimental approach is not straightforward as a diffuse coupling for mechanical systems requires access to the kinematic equation. Furthermore, the measure differential inclusion describing the dynamics of the system is transformed to a measure differential equation before the coupling is applied. This approach is feasible for a computer simulation, but not for a physical system such as a mechanical system including Coulomb friction.

# Acknowledgments

# References

[1] AGENO, A., AND SINOPOLI, A. Lyapunov's exponents for nonsmooth dynamics with impacts: Stability analysis of the rocking block. *International Journal of Bifurcation and Chaos 15*, 6 (2005), 2015–2039.

[2] AIZERMAN, M. A., AND GANTMAKHER, F. R. On the stability of periodic motions. *Journal of Applied Mathematics and Mechanics (translated from Russian) 1* (1958), 1065–1078.

[3] ARENAS, A., DÍAZ-GUILERA, A., KURTHS, J., MORENO, Y., AND ZHOU, C. Synchronization in complex networks. *Physics Reports 469*, 3 (2008), 93–153.

[4] BARREIRA, L., AND PESIN, Y. B. *Lyapunov Exponents and Smooth Ergodic Theory.* American Mathematical Society, Providence, Rhode Island, 2002.

[5] BENETTIN, G., GALGANI, L., GIORGILLI, A., AND STRELCYN, J. M. Lyapunov characteristic exponents for smooth dynamical systems and for Hamiltonian systems; A method for computing all of them. Part 1: Theory. *Meccanica 15*, 1 (1980), 9–20.

[6] BENETTIN, G., GALGANI, L., GIORGILLI, A., AND STRELCYN, J. M. Lyapunov characteristic exponents for smooth dynamical systems and for Hamiltonian systems; A method for computing all of them. Part 2: Numerical application. *Meccanica 15*, 1 (1980), 21–30.

[7] BOCKMAN, S. F. Lyapunov exponents for systems described by differential equations with discontinuous right-hand sides. *Proceedings of the American Control Conference* (1991), 1673–1678.

[8] BOGACHEV, V. I. *Measure Theory.* Springer, Berlin Heidelberg, 2007.

[9] BROGLIATO, B. *Nonsmooth Mechanics. Models, Dynamics and Control*, 2 ed. Communications and Control Engineering. Springer-Verlag, London, 1999.

[10] DI BERNARDO, M., BUDD, C. J., CHAMPNEYS, A. R., KOWALCZYK, P., NORDMARK, A. B., TOST, G. O., AND PIIROINEN, P. T. Bifurcations in nonsmooth dynamical systems. *SIAM Review 50*, 4 (2008), 629–701.

[11] ECKMANN, J. P., AND KAMPHORST, S. O. Liapunov exponents from time series. *Physical Review A 34*, 6 (1986), 4971–4979.

[12] ECKMANN, J. P., AND RUELLE, D. Ergodic theory of chaos and strange attractors. *Reviews of Modern Physics 57* (1985), 617–656.

[13] ELSTRODT, J. *Maß- und Integrationstheorie*, 2 ed. Springer-Verlag, Berlin, Heidelberg, New York, 1999.

[14] FU, S., AND WANG, Q. Estimating the largest Lyapunov exponent in a multibody system with dry friction by using chaos synchronization. *Acta Mechanica Sinica 22*, 3 (2006), 277–283.

[15] FUJISAKA, H., AND YAMADA, T. Stability theory of synchronized motion in coupled-oscillator systems. *Progress of Theoretical Physics 69*, 1 (1983), 32–47.

[16] FUJISAKA, H., AND YAMADA, T. Stability theory of synchronized motion in coupled-oscillator systems IV: Instability of synchronized chaos and new intermittency. *Progress of Theoretical Physics 75*, 5 (1986), 1087–1104.

[17] GENCAY, R., AND DECHERT, W. D. An algorithm for the n Lyapunov exponents of an n-dimensional unknown dynamical system. *Physica D: Nonlinear Phenomena 59*, 1 (1992), 142–157.

[18] GLOCKER, CH. *Set-Valued Force Laws, Dynamics of Non-Smooth Systems*, vol. 1 of *Lecture Notes in Applied Mechanics.* Springer-Verlag, Berlin, 2001.

[19] GUCKENHEIMER, J., AND HOLMES, P. *Nonlinear Oscillations, Dynamical Systems, and Bifurcations of Vector Fields*, vol. 42 of *Applied Mathematical Sciences.* Springer-Verlag, New York, 1983.

[20] HAKEN, H. At least one Lyapunov exponent vanishes if the trajectory of an attractor does not contain a fixed point. *Physics Letters A 94*, 2 (1983), 71–72.

[21] JORDAN, D. W., AND SMITH, P. *Nonlinear Ordinary Differential Equations: An Introduction for Scientists and Engineers*, 4 ed. Oxford University Press, Oxford, 2007.

[22] LEINE, R. I., AND BAUMANN, M. Variational analysis of inequality impact laws. In *Proceedings of the 8th EUROMECH Nonlinear Dynamics Conference (ENOC 2014)* (Vienna, Austria, 2014).

[23] LEINE, R. I., AND NIJMEIJER, H. *Dynamics and Bifurcations of Non-Smooth Mechanical Systems*, vol. 18 of *Lecture Notes in Applied and Computational Mechanics.* Springer-Verlag, Berlin, 2004.

[24] LEINE, R. I., AND VAN DE WOUW, N. *Stability and Convergence of Mechanical Systems with Unilateral Constraints*, vol. 36 of *Lecture Notes in Applied and Computational Mechanics*. Springer-Verlag, Berlin, 2008.

[25] MOON, F. C. *Chaotic Vibrations: An Introduction for Applied Scientists and Engineers*. John Wiley&Sons, New York, 1987.

[26] MOREAU, J. J. Bounded variation in time. In *Topics in Nonsmooth Mechanics*, J. J. Moreau, P. D. Panagiotopoulos, and G. Strang, Eds. Birkhäuser, Basel, Boston, Berlin, 1988, pp. 1–74.

[27] MOREAU, J. J. Unilateral contact and dry friction in finite freedom dynamics. In *Non-Smooth Mechanics and Applications*, J. J. Moreau and P. D. Panagiotopoulos, Eds., vol. 302 of *CISM Courses and Lectures*. Springer-Verlag, Wien, 1988, pp. 1–82.

[28] MÜLLER, P. C. Calculation of Lyapunov exponents for dynamic systems with discontinuities. *Chaos, Solitons & Fractals 5*, 9 (1995), 1671–1681.

[29] NAYFEH, A. H., AND BALACHANDRAN, B. *Applied Nonlinear Dynamics; Analytical, Computational, and Experimental Methods*. John Wiley & Sons, New York, 1995.

[30] NORDMARK, A. B. Universal limit mapping in grazing bifurcations. *Physical Review E 55*, 1 (1997), 266–270.

[31] OSELEDEC, V. I. A multiplicative ergodic theorem. Characteristic Ljapunov exponents of dynamical systems. (in russian). *Trudy Moskovskogo matematičeskogo obščestva 19* (1968), 179–210.

[32] OTT, W., AND YORKE, J. A. When Lyapunov exponents fail to exist. *Physical Review E 78*, 5 (2008), 056203.

[33] PAOLI, L. Continuous dependence on data for vibro-impact problems. *Mathematical Models and Methods in Applied Sciences 15*, 1 (2005), 53–93.

[34] PECORA, L. M., AND CARROLL, T. L. Master stability functions for synchronized coupled systems. *International Journal of Bifurcation and Chaos 9*, 12 (1998), 2315–2320.

[35] ROCKAFELLAR, R. T., AND WETS, R. J.-B. *Variational Analysis*. Springer-Verlag, Berlin, 1998.

[36] RUDIN, W. *Principles of Mathematical Analysis*, 3 ed. International series in pure and applied mathematics. McGraw-Hill, New York, 1976.

[37] RUELLE, D. Ergodic theory of differentiable dynamical systems. *Mathématiques de l'Institut des Hautes Études Scientifiques 50*, 1 (1979), 27–58.

[38] RUELLE, D. Sensitive dependence on initial conditions and turbulent behavior of dynamical systems. *Annals of the New York Academy of Sciences 316*, 1 (1979), 408–416.

[39] SANO, M., AND SAWADA, Y. Measurement of the Lyapunov spectrum from a chaotic time series. *Physical Review Letters 55* (1985), 1082–1085.

[40] SHIMADA, I., AND NAGASHIMA, T. A numerical approach to ergodic problem of dissipative dynamical systems. *Progress of Theoretical Physics 61*, 6 (1979), 1605–1616.

[41] STEFANSKI, A. Estimation of the largest Lyapunov exponent in systems with impacts. *Chaos, Solitons & Fractals 11*, 15 (2000), 2443–2451.

[42] STEFANSKI, A., AND KAPITANIAK, T. Estimation of the dominant Lyapunov exponent of non-smooth systems on the basis of maps synchronization. *Chaos, Solitons & Fractals 15*, 2 (2003), 233–244.

[43] STROGATZ, S. H. *Nonlinear Dynamics and Chaos with Application to Physics, Biology, Chemistry and Engineering.* Westview Press, Massachusetts, 1994.

[44] WOLF, A., SWIFT, J. B., SWINNEY, H. L., AND VASTANO, J. A. Determining Lyapunov exponents from a time series. *Physica D: Nonlinear Phenomena 16*, 3 (1985), 285–317.

[45] YAMADA, T., AND FUJISAKA, H. Stability theory of synchronized motion in coupled-oscillator systems II: The mapping approach. *Progress of Theoretical Physics 70*, 5 (1983), 1240–1248.

[46] YAMADA, T., AND FUJISAKA, H. Stability theory of synchronized motion in coupled-oscillator systems III: Mapping model for continuous system. *Progress of Theoretical Physics 72*, 5 (1984), 885–894.